Neutron Star Mass and Radius Measurements

J. M. Lattimer

Department of Physics & Astronomy
STONY BROOK UNIVERSITY

U.S. DEPARTMENT OF ENERGY Office of Science

N3AS

CSQCD VII
CUNY Advanced Science Research Center
11-15 June, 2018

Neutron Star Mass and Radius Measurements

- Nuclear theory and experiment
- Photospheric Radius Expansion Bursts
- Quiescent Low-Mass X-ray Binaries
- Pulsar Timing
- GW170817

Neutron Star Radii and Nuclear Symmetry Energy

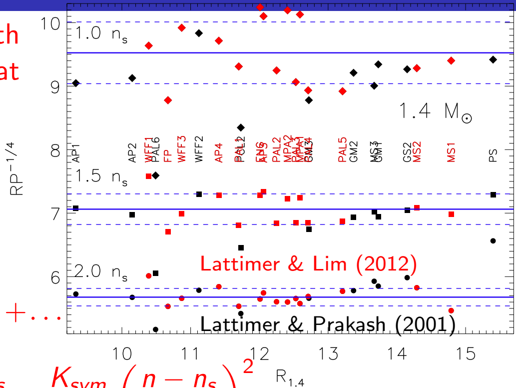

- Radii are highly correlated with neutron star matter pressure at $1 - 2n_s \simeq 0.16 - 0.32$ fm^{-3}.
- Neutron star matter is nearly pure neutrons, $x \sim 0.04$.
- Nuclear symmetry energy

$$S(n) \equiv E_0(n) - E_{1/2}(n)$$

$$E_x(n) \simeq E_{1/2}(n) + S_2(n)(1-2x)^2 + \dots$$

$$S(n) \simeq S_2(n) \simeq S_v + \frac{L}{3}\frac{n-n_s}{n_s} + \frac{K_{sym}}{18}\left(\frac{n-n_s}{n_s}\right)^2 \dots$$

- $S_v \equiv S_2(n_s) \sim 32$ MeV, $L \sim 50$ MeV; nuclear systematics.
- Neutron matter energy and pressure at n_s:

$$E_0(n_s) \simeq S_v + E_{1/2}(n_s) = S_v - B \sim 13 - 17 \text{ MeV}$$

$$p_0(n_s) = \left(n^2 \frac{\partial E_0(n)}{\partial n}\right)_{n_s} \simeq \frac{L n_s}{3} \sim 2.1 - 3.7 \text{ MeV fm}^{-3}$$

Causality + GR Limits and the Maximum Mass

A lower limit to the maximum mass sets a lower limit to the radius for a given mass.

Similarly, a precision upper limit to R sets an upper limit to the maximum mass.

$R_{1.4} > 8.15(10.9)$ km if $M_{max} \geq 2.01 M_\odot$.

$M_{max} < 3.0(2.3)\ M_\odot$ if $R < 13$ km.

$M - R$ curves for maximally compact EOS

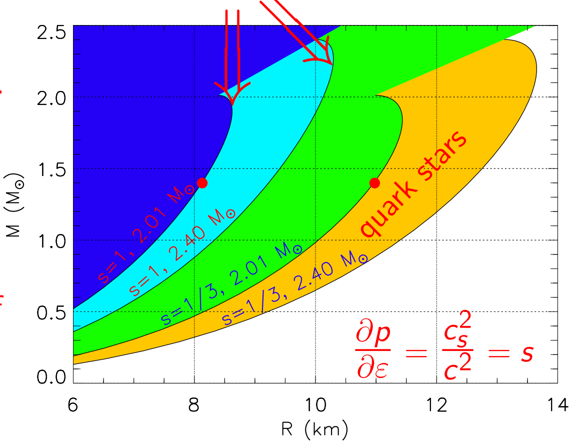

If quark matter exists in the interior, the minimum radii are substantially larger; maximum masses are considerably smaller.

Unitary Gas Bounds

Neutron matter energy should be larger than the unitary gas energy $E_{UG} = \xi_0 (3/5) E_F$

$$E_{UG} = 12.6 \left(\frac{n}{n_s}\right)^{2/3} \mathrm{MeV}$$

(Tews et al. 2017).

The unitary gas refers to fermions interacting via a pairwise short-range s-wave interaction with an infinite scattering length and zero range. Cold atom experiments show a universal behavior with the Bertsch parameter $\xi_0 \simeq 0.37$.

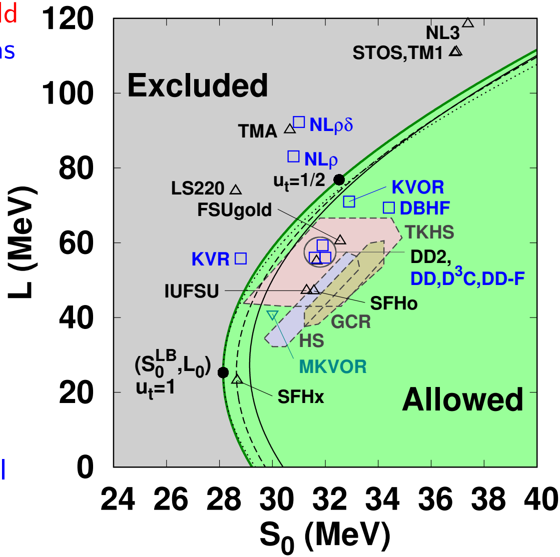

$S_v \geq 28.6$ MeV; $L \geq 25.3$ MeV; $p_0(n_s) \geq 1.35$ MeV fm^{-3}; $R_{1.4} \geq 9.7$ km

Theoretical and Experimental Constraints

H Chiral Lagrangian

G: Quantum Monte Carlo

neutron matter constraints from Hebeler et al. (2012)

unitary gas constraints from Tews et al. (2017)

Experimental constraints are compatible with unitary gas bounds.

Neutron matter constraints are compatible with experimental constraints.

$$10.9 \text{ km} \leq R_{1.4} \leq 13.1 \text{ km}$$

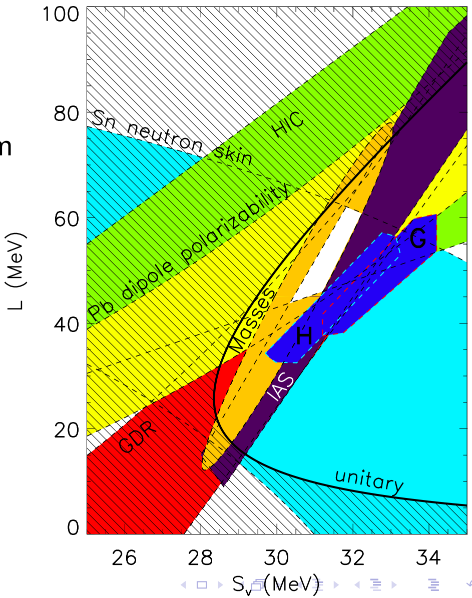

Constraints Using Piecewise Polytropes

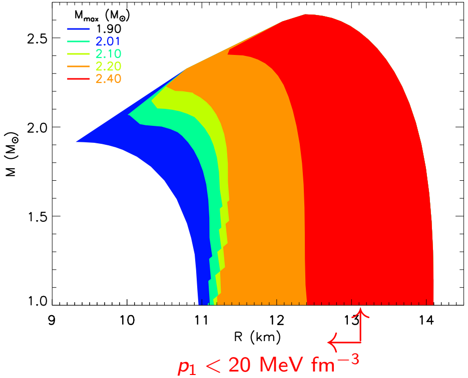

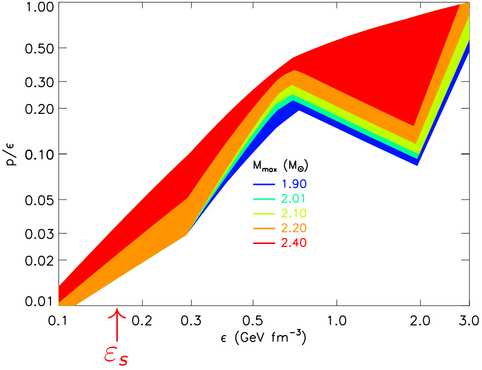

Simultaneous Mass/Radius Measurements

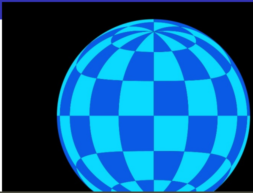

- Measurements of flux $F_\infty = (R_\infty/D)^2 \sigma T_{\rm eff}^4$ and color temperature $T_c \propto \lambda_{\rm max}^{-1}$ yield an apparent angular size (pseudo-BB):

$$R_\infty/D = (R/D)/\sqrt{1 - 2GM/Rc^2}$$

- Observational uncertainties include distance D, nonuniform T, interstellar absorption N_H, atmospheric composition

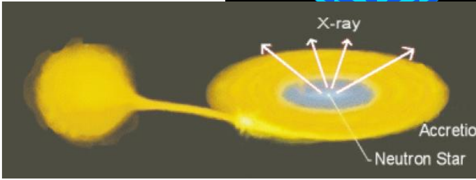

Best chances are:

  - Isolated neutron stars with parallax (atmosphere ??)
  - Quiescent low-mass X-ray binaries (QLMXBs) in globular clusters (reliable distances, low B H-atmosperes)
  - Bursting sources with peak fluxes close to Eddington limit (PREs); gravity balances radiation pressure

$$F_{\rm Edd} = \frac{cGM}{\kappa D^2}\sqrt{1 - 2GM/Rc^2}$$

Photospheric Radius Expansion X-Ray Bursts

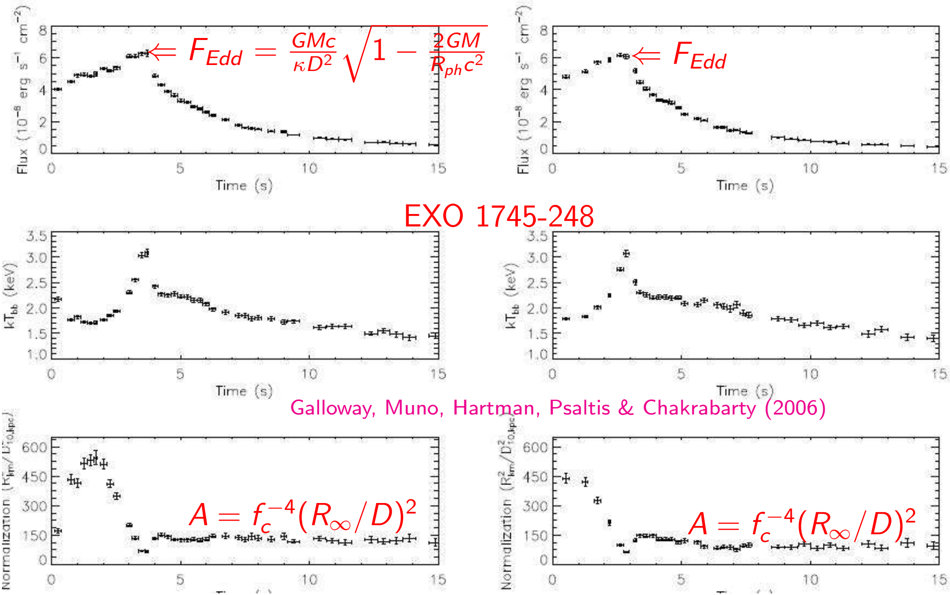

PRE Burst Models

Ozel et al. $z_{\rm ph} = z$ $\quad \beta = GM/Rc^2$

$$F_{\rm Edd} = \frac{GMc}{\kappa D}\sqrt{1-2\beta}$$

$$A = \frac{F_\infty}{\sigma T_\infty^4} = f_c^{-4}\left(\frac{R_\infty}{D}\right)^2$$

$$\alpha = \frac{F_{\rm Edd}}{\sqrt{A}}\frac{\kappa D}{F_c^2 c^3} = \beta(1-2\beta)$$

$$\gamma = \frac{Af_c^4 c^3}{\kappa F_{\rm Edd}} = \frac{R_\infty}{\alpha}$$

$$\beta = \frac{1}{4} \pm \frac{1}{4}\sqrt{1-8\alpha}$$

$$\alpha \le \frac{1}{8} \text{ required.}$$

Steiner et al. $z_{\rm ph} << z$

$$F_{\rm Edd} = \frac{GMc}{\kappa D}$$

$$\alpha = \beta\sqrt{1-2\beta}$$

$$\theta = \cos^{-1}\left(1-54\alpha^2\right)$$

$$\beta = \frac{1}{6}\left[1+\sqrt{3}\sin\left(\frac{\theta}{3}\right) - \cos\left(\frac{\theta}{3}\right)\right]$$

$$\alpha \le \sqrt{\frac{1}{27}} \simeq 0.192 \text{ required.}$$

EXO1745-248	4U1608-522	4U1820-30	KS1731-260	SAXJ1748.9-2021
0.19 ± 0.04	0.25 ± 0.06	0.24 ± 0.04	0.20 ± 0.03	0.18 ± 0.04

observed α values (Ozel et al.)

PRE $M - R$ Estimates

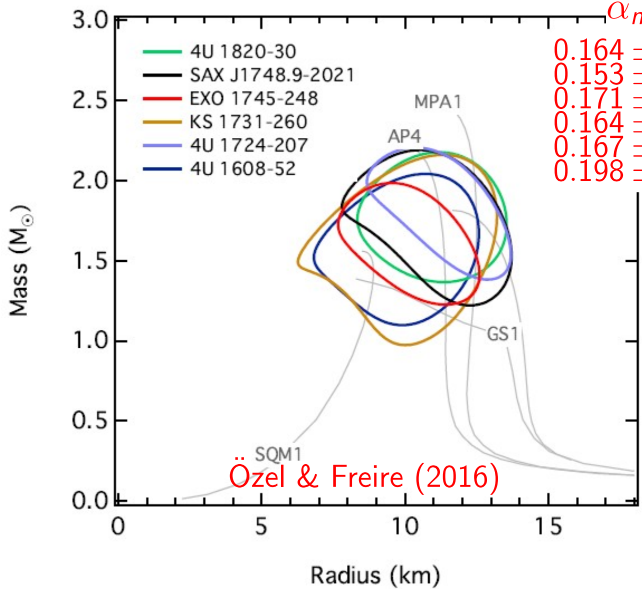

α_{min}

0.164 ± 0.024
0.153 ± 0.039
0.171 ± 0.042
0.164 ± 0.037
0.167 ± 0.045
0.198 ± 0.047

QLMXBs (Guillot & Rutledge 2013)

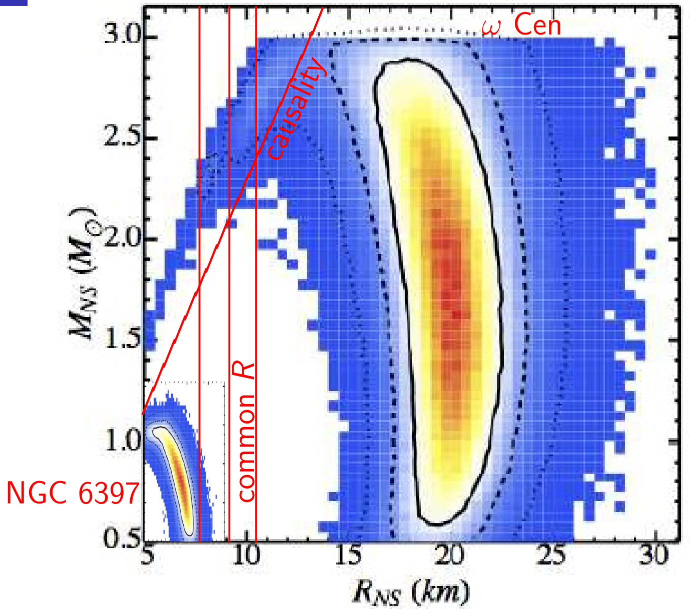

Guillot & Rutledge (

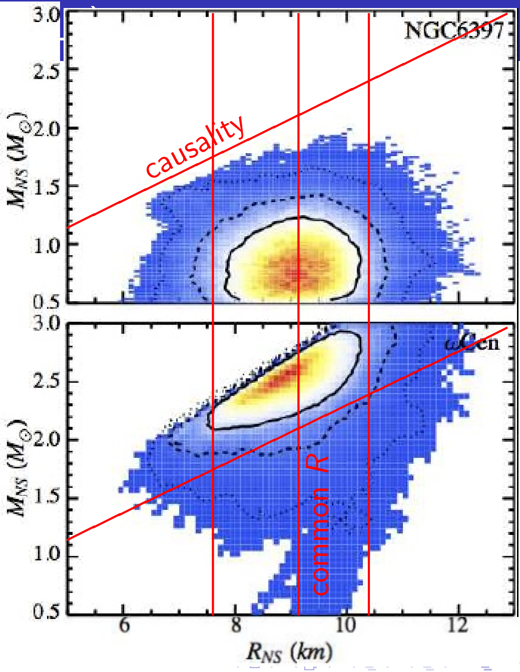

QLMXB $M - R$ Estimates

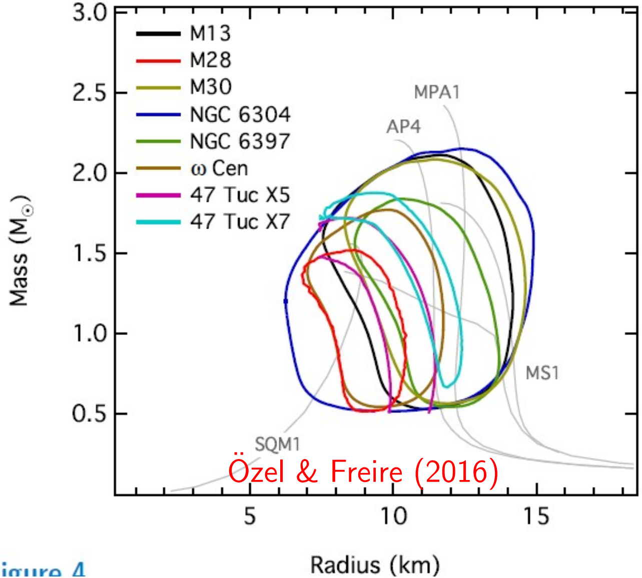

igure 4

M13 QLMXB (Shaw et al. 2018)

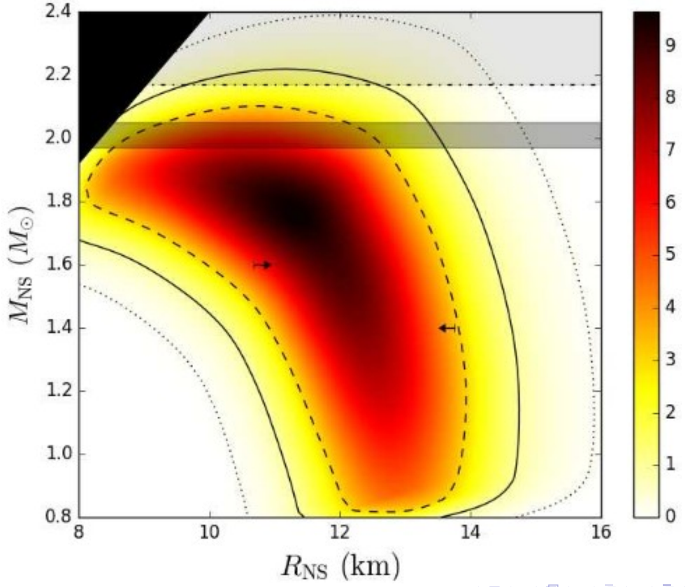

8 QLMXBs (Steiner et al. 2018)

Parameterized EOS priors

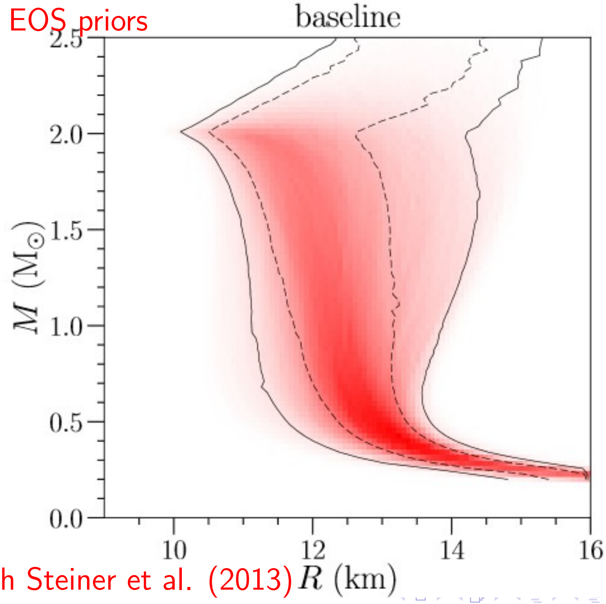

Consistent with Steiner et al. (2013)

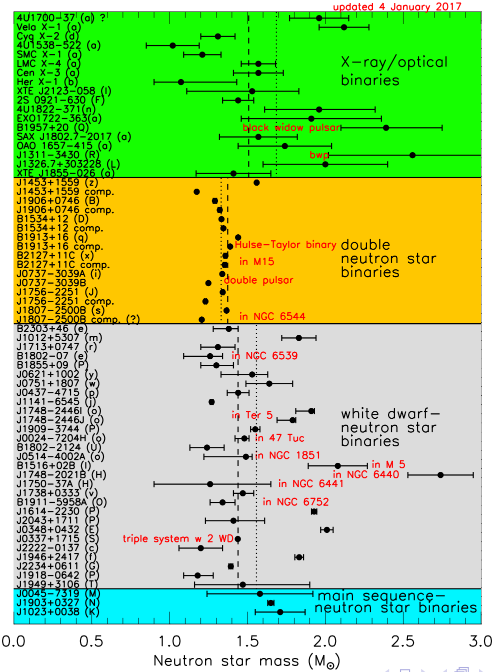

vanKerkwijk 2010

Romani et al. 2012

Although simple average mass of w.d. companions is 0.23 $M_\odot$ larger, weighted average is 0.04 $M_\odot$ smaller

Demorest et al. 2010
Fonseca et al. 2016
Antoniadis et al. 2013
Barr et al. 2016

Champion et al. 2008

Black Widow Pulsar PSR B1957+20

A 1.6ms pulsar in circular 9.17h orbit with $\sim 0.03\ M_\odot$ companion.

The pulsar is eclipsed for 50-60 minutes each orbit; eclipsing object has a volume much larger than the secondary or its Roche lobe.

Pulsar is ablating the companion leading to mass loss and the eclipsing plasma. The secondary may nearly fill its Roche lobe.

Ablation by the pulsar leads to secondary's eventual disappearance.

The optical light curve tracks the motion of the secondary's irradiated hot spot rather than its center of mass motion.

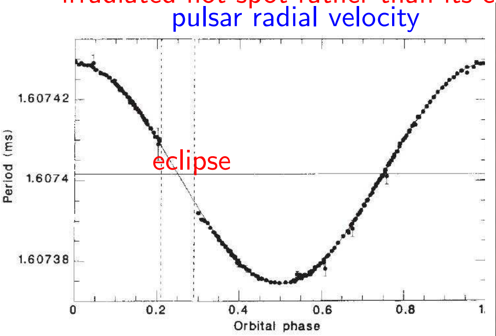

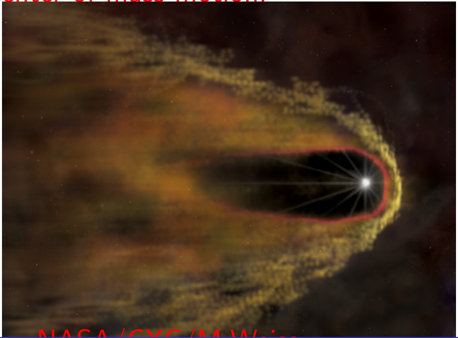

PSR J2215-5135

- Redback binary MSP
- $P_{orb} = 4.14$ hr
- $T_{night} = 5660^{+260}_{-380}$ K
- $T_{day} = 8080^{+470}_{-280}$ K
- D $= 2.9 \pm 0.1$ kpc
- $e = 0.144 \pm 0.002$
- Roche lobe filling factor $f = 0.95 \pm 0.01$
- $M_{pulsar} = 2.27^{+0.17}_{-0.15} M_\odot$
- $M_{comp} = 0.33^{+0.02}_{-0.02} M_\odot$

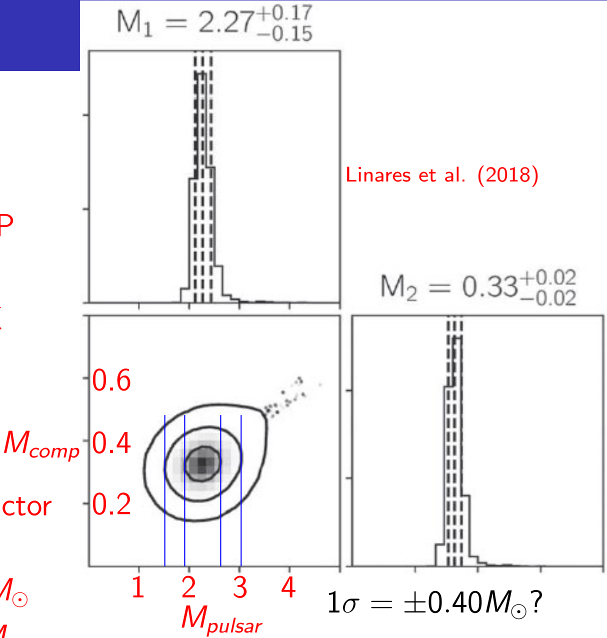

GW170817

- LIGO-Virgo detected signal consistent with a BNS merger, followed 1.7 s later by a weak sGRB.
- 1500 orbits observed over 100 s.
- Chirp mass $\mathcal{M}_{\rm chirp} = 1.19 M_\odot$
- $M_{\rm tot,max} = 2^{6/5}\mathcal{M}_{\rm chirp} = 2.73 M_\odot$
- $E_{\rm rad} > 0.025 M_\odot c^2$
- $D_L = 40 \pm 10$ Mpc
- $\tilde\Lambda < 1050$ (90%)
- $M_{\rm ejecta} \sim 0.05 \pm 0.01 \; M_\odot$
- Blue ejecta: $\sim 0.01 M_\odot$
- Red ejecta: $\sim 0.05 M_\odot$
- Likely r-process production

Properties of Double Neutron Star Binaries

DNS with only an upper limit to m_p

DNS with $\tau_{GW} = \infty$

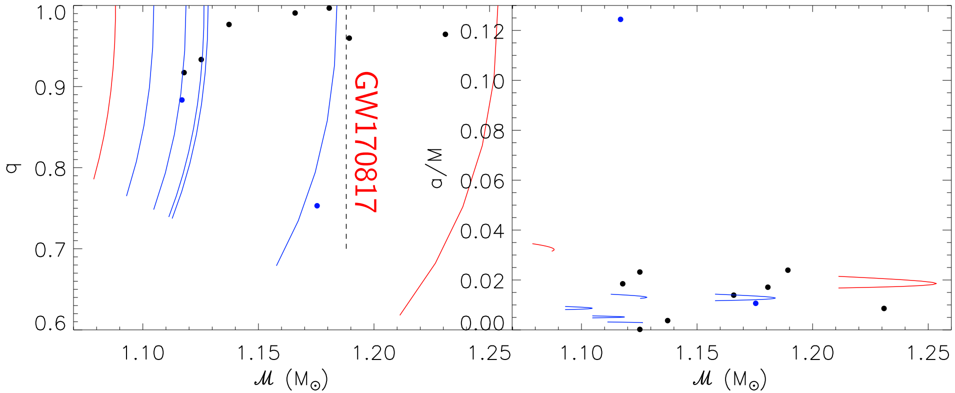

LIGO/VIRGO (2017) Parameter Determination

There are 11 free wave-form parameters to the lowest post-Newtonian order including finite-size effects, LV17 used a 13 parameter model fitting to one higher PN order:

Extrinsic:

- Sky location (2)
- Distance (1)
- Inclination (1)
- Coalescence time (1)
- Coalescence phase (1)
- Polarization (1)

Intrinsic:

- Component masses (2)
- Spin parameters (2)
- Tidal parameters (2)

Deformability and the Radius

- $\Lambda = a(Rc^2/GM)^6$
  $a = 0.0093 \pm 0.0007$ for
  $M = 1.35 \pm 0.25\ M_\odot$

$$\tilde{\Lambda} = \frac{16}{13}\frac{(1+12q)\Lambda_1 + q^4(12+q)\Lambda_2}{(1+q)^5}$$

- $R_1 \simeq R_2 \simeq \hat{R}$

$$\tilde{\Lambda} \simeq \frac{16a}{13}\left(\frac{\hat{R}c^2}{G\mathcal{M}}\right)^6 \frac{q^{8/5}(12-11q+12q^2)}{(1+q)^{26/5}}$$

- $\tilde{\Lambda} = a'(\hat{R}c^2/G\mathcal{M})^6$
  $a' = 0.0042 \pm 0.0004$ for
  $\mathcal{M} = 1.1 \pm 0.2\ M_\odot$

- $\hat{R} = 11.2 \pm 0.2\ \frac{\mathcal{M}}{M_\odot}\left(\frac{\tilde{\Lambda}}{800}\right)^{1/6}$ km

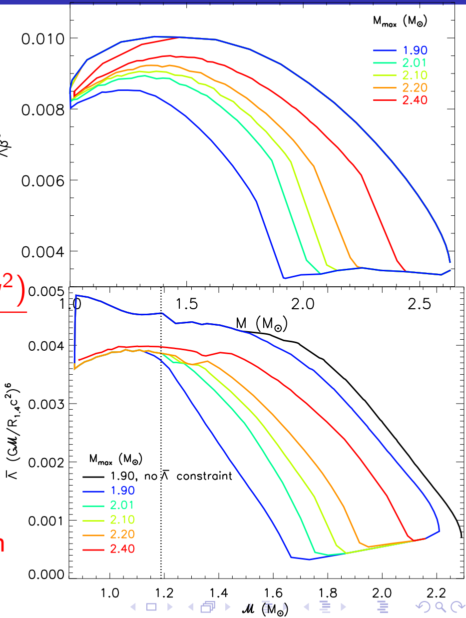

Tidal Deformabilities

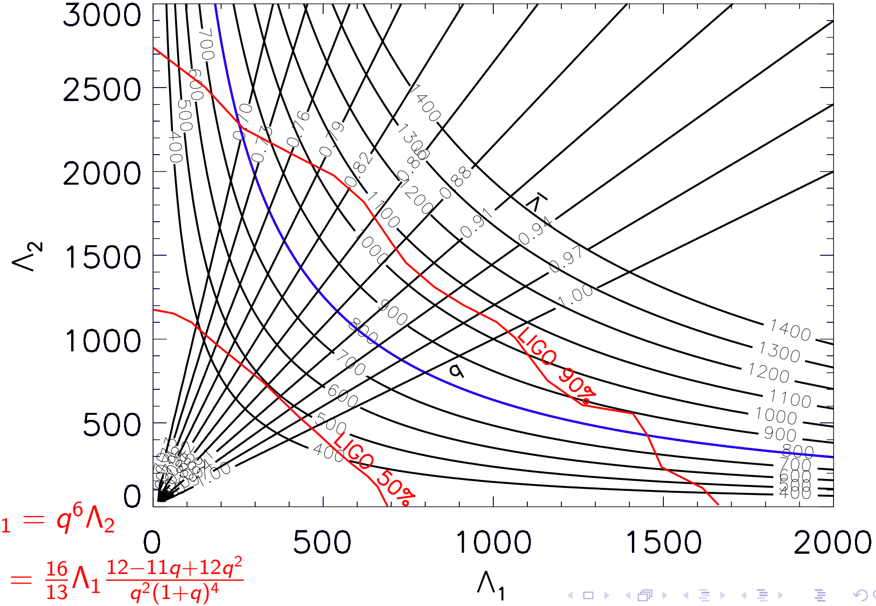

$\Lambda_1 = q^6 \Lambda_2$

$\tilde{\Lambda} = \frac{16}{13}\Lambda_1 \frac{12-11q+12q^2}{q^2(1+q)^4}$

It's Important to Include $\Lambda_1 - \Lambda_2$ Correlations

- LV17 did not consider these correlations, i.e., the stars were not assumed to have the same EOS.
- Their priors on Λ_1, Λ_2 included $\Lambda_1 > \Lambda_2$, which is physically implausible and biases results.
  $(c^2/G)dR/dM \geq 1$ for $m_2 \leq M \leq m_1$, $\Lambda_1 \leq \Lambda_2$.
  Piecewise polytrope analysis finds $(c^2/G)dR/dM \leq 0.26$.
- Correlating Λ_1 and Λ_2 reduces the estimated $\tilde{\Lambda}$ by $\sim 20\%$; checked by MC analysis using $\Lambda_1 = q^6\Lambda_2$.
- The lower bound to $\Lambda(M)$ from causality and unitary gas constraints should be included: $\Lambda(M = 1.4M_\odot) \gtrsim 90$.
- Proposed upper bounds to $\Lambda(M)$ from causality (Friedmann et al. 2017) are model-dependent.

A Re-Analysis of GW170817, De et al. (2018)

- De18 takes advantage of the precisely-known electro-magnetic source position (Soares-Santos et al., 2017).
- Uses existing knowledge of the H_0 and the redshift of NGC 4993 to fix the distance (Cantiello et al., 2017).
- Assumes both neutron stars have the same equation of state by determining and using a correlation among m_1, m_2, Λ_1 and Λ_2: $\Lambda_1 = q^6 \Lambda_2$.
- The baseline model thus has 9 instead of 13 parameters.
- Explores effects of varying mass and deformability priors.
- Explores effects of neglecting deformability correlations and/or component spins.
- Shows substantial evidence for a common EOS.
- Confirms a common EOS reduces $\tilde{\Lambda}$ estimate by $\sim 20\%$.
- Determines 90% lower confidence bounds to Λ_1, Λ_2 and $\tilde{\Lambda}$.
- Shows more evidence for tidal effects than for spins.

De18 GW170817 Baseline Results for $\Lambda_1 - \Lambda_2$

Uncertainties reflect 90% credible intervals

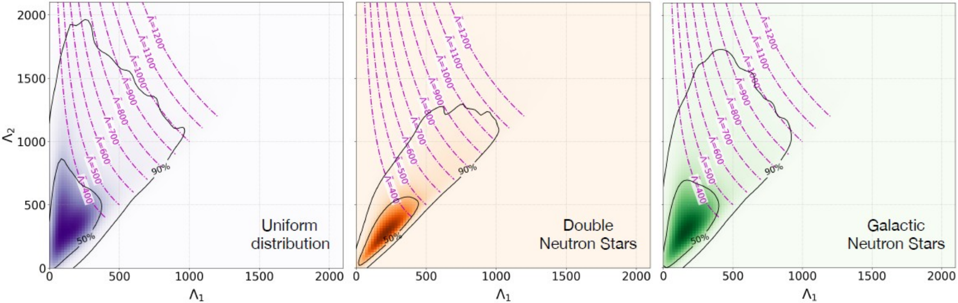

Uniform	Double Neutron Stars	Galactic Neutron Stars
$\bar{\Lambda} = 310^{+679}_{-234}$	$\bar{\Lambda} = 354^{+691}_{-245}$	$\bar{\Lambda} = 334^{+670}_{-241}$
$\bar{\Lambda} < 825$ (90%)	$\bar{\Lambda} < 852$ (90%)	$\bar{\Lambda} < 888$ (90%)
$\bar{\Lambda} > 125$ (90%)	$\bar{\Lambda} > 170$ (90%)	$\bar{\Lambda} > 140$ (90%)
$\mathcal{B} = 250$	$\mathcal{B} = 110$	$\mathcal{B} = 97$

$\mathcal{B}$ is Bayes Factor relative to runs with uncorrelated Λ's.

Evidence against strong phase transition for $1.1 - 1.6 M_\odot$.

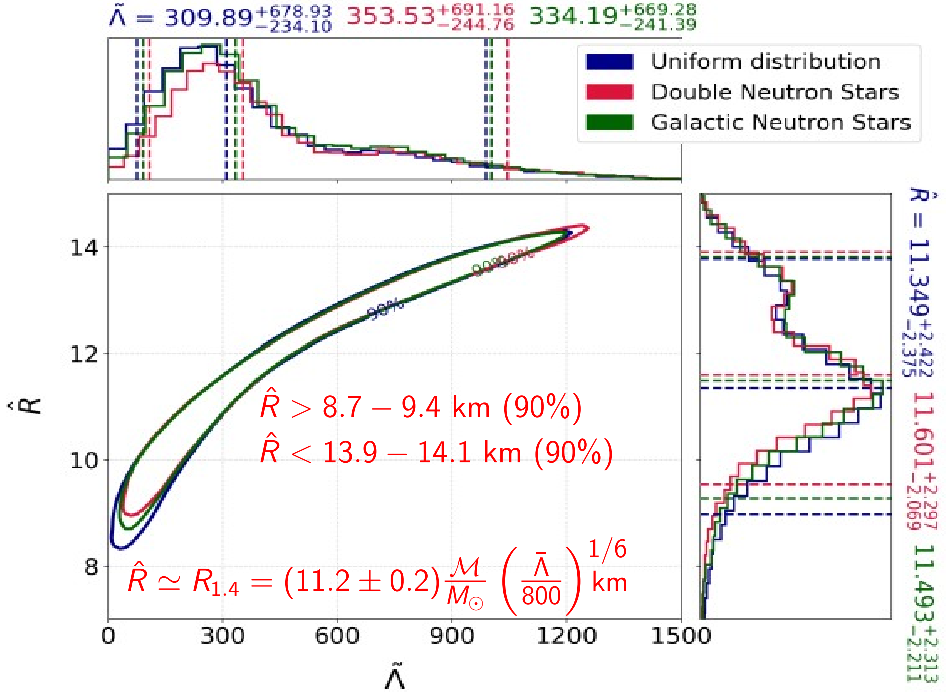
$\tilde{\Lambda} = 309.89^{+678.93}_{-234.10}$ $353.53^{+691.16}_{-244.76}$ $334.19^{+669.28}_{-241.39}$
Uniform distribution
Double Neutron Stars
Galactic Neutron Stars
$\hat{R} = 11.349^{+2.422}_{-2.375}$ $11.601^{+2.297}_{-2.069}$ $11.493^{+2.313}_{-2.211}$
90%
$\hat{R}$
$\tilde{\Lambda}$
0
300
600
900
1200
1500
8
10
12
14
$\hat{R} > 8.7 - 9.4$ km (90%)
$\hat{R} < 13.9 - 14.1$ km (90%)
$\hat{R} \simeq R_{1.4} = (11.2 \pm 0.2)\frac{\mathcal{M}}{M_\odot}\left(\frac{\bar{\Lambda}}{800}\right)^{1/6}$ km

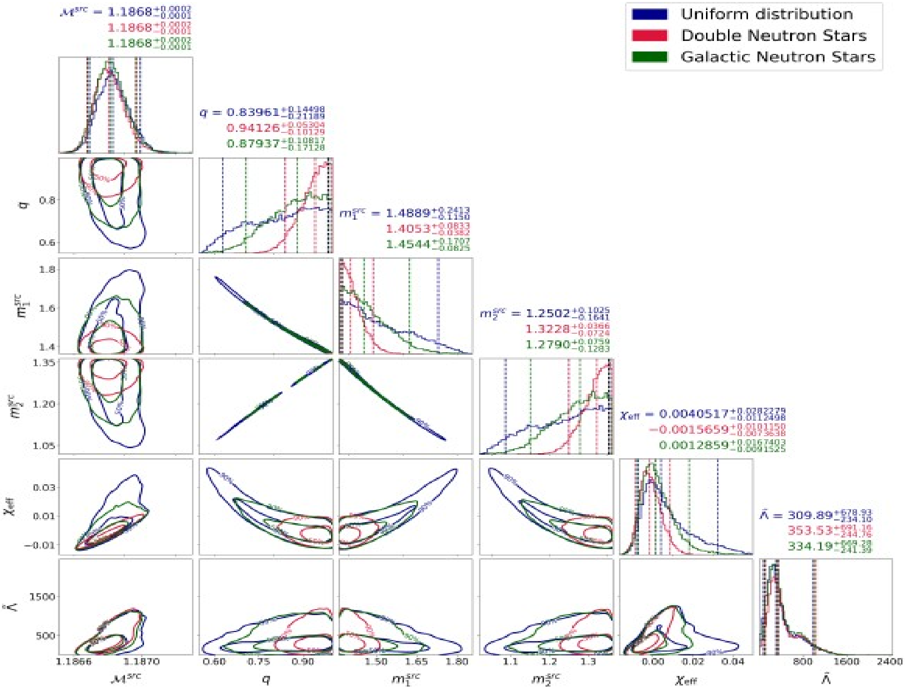
Uniform distribution
Double Neutron Stars
Galactic Neutron Stars

Comparison of De18 and LV17 for Uncorrelated Λ's

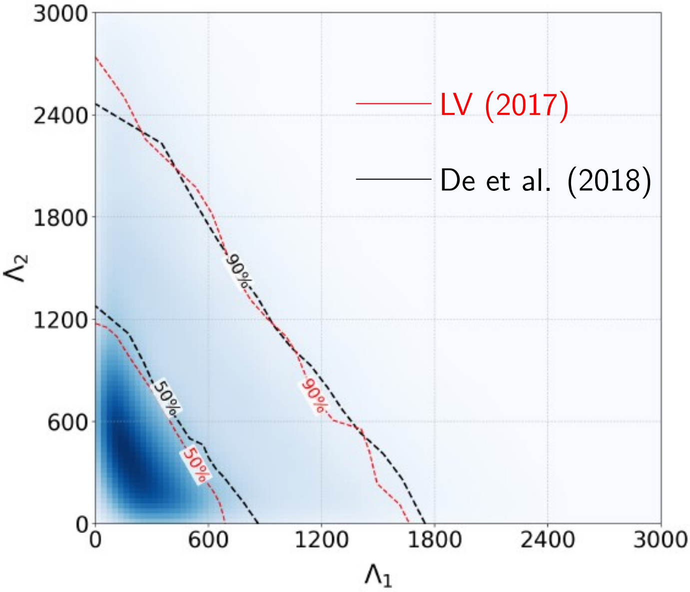

Comparison with LIGO/VIRGO (2018) Reanalysis

LV18 considered

- different waveform models,
- newer cleaned data,
- recalibrated VIRGO detector,
- EM source position,
- lower f_{low} cutoff,
- a common EOS.

It's been suggested a 4-parameter spectral decomposition EOS is superior to a 3-segment piecewise polytrope EOS for inferring deformabilities. However,

- LV18 does not vary EOS parameters over the entire ranges permitted by causality, $M_{max} \geq 1.97 M_\odot$, and thermodynamic stability (Lindblom 2010);
- Assuming flat priors for the 4 EOS parameters result in Gaussian-like Λ priors, with bias toward central values;
- Spectral decomposition de-emphasizes sudden sound speed changes, including phase transitions, thus does not sample as wide a range of $p - \varepsilon$ and $M - R$ variations.
- Complete coverage of possible configurations, not accuracy, is more important for establishing correlations.

LV18 Validated $R_1 \simeq R_2$ for GW170817

$\Lambda_2 - \Lambda_1$ correlations from parameterized EOSs with $M_{max} > 1.97 M_\odot$

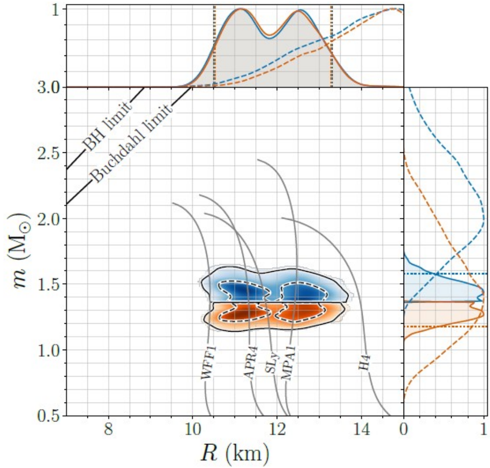

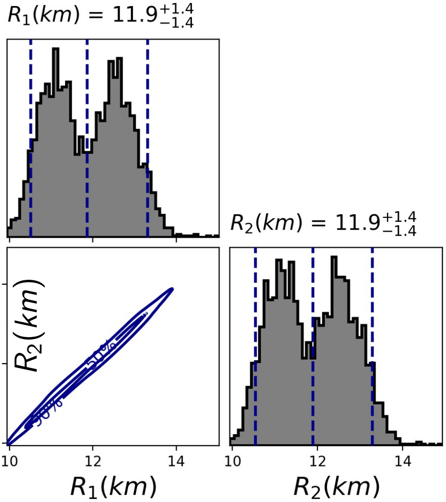

LV18

GW Summary

- LV18: common EOS and source position assumptions reduce $\tilde{\Lambda}$ by about 20%, confirming De18 results.
- LV18: Better waveform models, compared to TaylorF2, reduce the 90% confidence upper limit to $\tilde{\Lambda}$ by an average of about 15%, consistent with earlier findings.
- LV18: $\tilde{\Lambda} \sim 260^{+320}_{-190}$, reduced by 40% from LV17.
- I infer $R_{1.4} \sim 11.0^{+1.8}_{-2.3}$ km; LV18 state $11.9^{+1.4}_{-1.4}$ km.
- The remaining $\sim 5\%$ reduction in Λ due to cleaned data, low-frequency cutoff, or deformability correlation method.
- LV18 report an approximate 50% reduction in uncertainties in $\tilde{\Lambda}$ and $R_{1.4}$ compared to De18.
  - Largely due to overall reduction in $\tilde{\Lambda}$ estimate.
  - Partially due to LV18 correlation method which biases towards central values of the correlation and $\tilde{\Lambda}$.
- Upper limit to M_{max} does not affect De18 results but will systematically decrease LV18 $\tilde{\Lambda}$ estimates.